Supporting Information for

Chiral Tetrahedral Iron(II) Cages: Diastereoselective Subcomponent Self-Assembly, Structure Interconversion and Spin-Crossover Properties

*Dong-Hong Ren, Dan Qiu, Chun-Yan Pang, Zaijun Li and Zhi-Guo Gu**

The Key Laboratory of Food Colloids and Biotechnology, Ministry of Education, School of Chemical and Material Engineering, Jiangnan University, Wuxi 214122, P.R. China

E-mail: zhiguogu@jiangnan.edu.cn

Table of contents

1. Experimental Section

All reagents and solvents were reagent grade, purchased from commercial sources and used without further purification. *Caution:* The perchlorate salts are potentially explosive. Thus, these starting materials should be handled in small quantities and with great caution. Infrared spectra were measured on an ABB Bomem FTLA 2000-104 spectrometer with KBr pellets in the 400-4000 cm^{-1} region. NMR spectra were recorded on AVANCE III (400 MHz) instrument at 298 K using standard Varian or Bruker software, and chemical shifts were reported in parts per milion (ppm) downfield from tetramethylsilane. Element analyses were conducted on elementar corporation vario EL III analyzer. UV/vis absorbance spectra were collected on Shimadzu UV-2101 PC scanning spectrophotometer. Circular dichroism (CD) spectra was carried out using a MOS-450/AF-CD spectro polarimeter at room temperature, which was calibrated conventionally using 0.060% ACS for intensity and a holmium filter for wavelength. The TG curves were carried out by using TGA/1100SF thermo grabinetric analyzer with a temperature range of 25 °C-600 °C. Variable-temperature magnetic susceptibility on polycrystalline samples were performed on a Quantum Design MPMS-XL-7 SQUID magnetometer over the temperature range 2–400 K at 1000 Oe. The molar susceptibility was corrected for diamagnetic contributions using Pascal's constants and the increment method.

2. Synthesis of 1,4-di(imidazole-2-carboxaldehyde)butane

imidazole-2-carboxaldehyde (1.3453 g, 14 mmol), 1,4-dibromobutane (1.0797 g, 5 mmol), and potassium carbonate (1.3821 g, 10 mmol) were added to a 50 mL flask containing 20 mL DMF in nitrogen atmosphere. The reaction mixture was stirred at 50 °C for 3 days and then filtered. The filtrate was extracted with ethyl acetate (4 × 10 mL), collecting the organic phase, washed with saturated aqueous solution of potassium chloride, dried with anhydrous magnesium sulfate, removed the solvent on a rotary evaporator and dried under vacuum in 40 °C to give 1.3106 g of the desired

product as yellow crystals (Yield: 82.67%). Pure light yellow crystals of 1,4-di(imidazole-2-carboxaldehyde)butane were obtained by recrystallizing the crude product from ethyl acetate. Anal. Calcd for $C_{12}H_{14}N_4O_2$: C, 58.53; H, 5.73; N, 22.75; Found: C, 58.50; H, 5.72; N, 22.79. IR (KBr, ν cm^{-1}): 3130, 2946, 2858, 1678, 1479, 1411, 1336, 770. ^{1}HNMR (400MHz: CD_3CN, δppm, Figure. S1): 9.705 (s, 2H^1), 7.350 (s, 2H^2), 7.233 (s, 2H^3), 4.395 (t, J = 6.4 Hz, 4H^4), 1.756 (m, 4H^5). ^{13}CNMR (400 MHz: CD_3CN, δppm, Figure. S2): 181.670, 130.888, 126.775, 116.997, 46.308, 27.159.

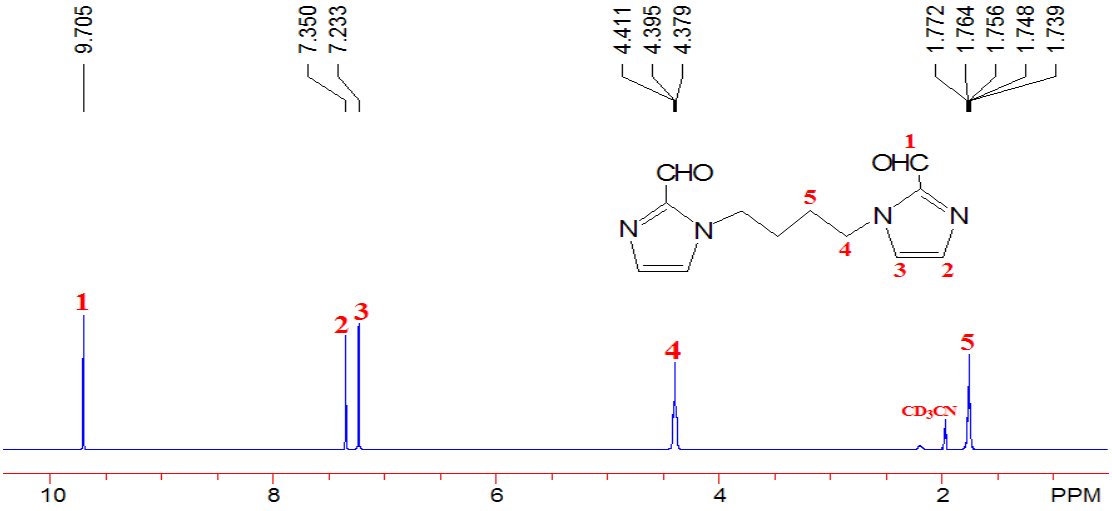

Fig. S1 ^{1}H NMR spectrum of 1,4-di(imidazole-2-carboxaldehyde)butane.

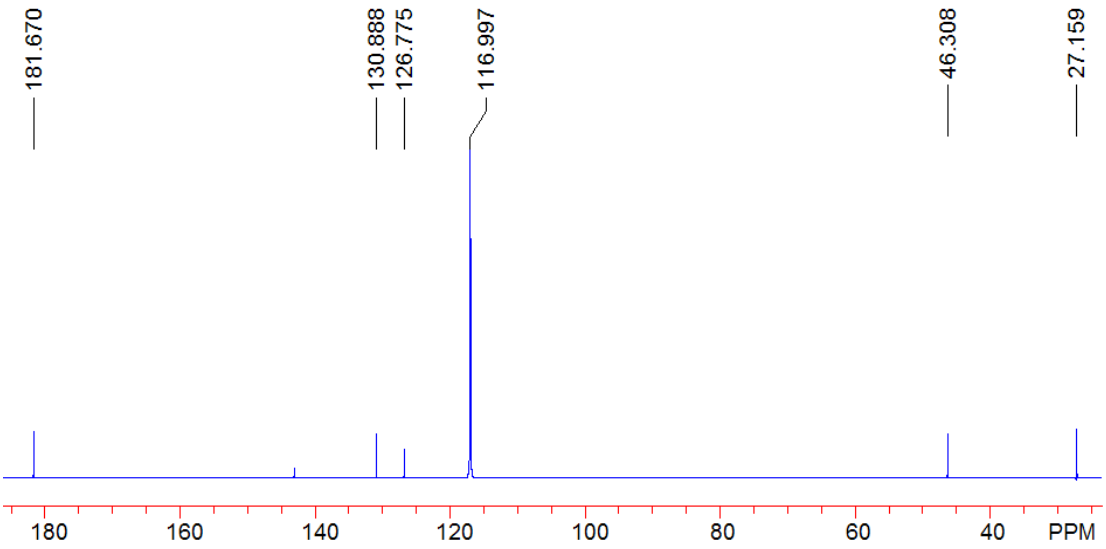

Fig. S2 ^{13}C NMR spectrum of 1,4-di(imidazole-2-carboxaldehyde)butane.

3. Synthesis of cage (*R*)-1 and (*S*)-1

1,4-di(imidazole-2-carboxaldehyde)butane (49.2 mg, 0.2 mmol), (*R*)- or (*S*)-1-phenylethylamine (48.9 mg, 0.4 mmol) and $Fe(ClO_4)_2 \cdot 6H_2O$ (48.4 mg, 0.13 mmol) were added to a flask with 10 mL of acetonitrile in nitrogen atmosphere. The solution was heated at 80 °C for 2 h, cooled to room temperature, the resulting purple solution was filtered. Cage **1** was precipitated as purple crystals through slow diffusion of diethyl ether into the filtrate at room temperature. Yield: 75%. Calcd for **(*R*)-1** $C_{168}H_{192}Cl_8Fe_4N_{36}O_{32} \cdot Et_2O \cdot 2MeCN \cdot H_2O$: C, 54.08; H, 5.42; N, 13.62; Found: C, 54.48; H, 5.51; N, 13.29. Calcd for **(*S*)-1** $C_{168}H_{192}Cl_8Fe_4N_{36}O_{32} \cdot Et_2O \cdot 2MeCN \cdot H_2O$: C, 54.08; H, 5.42; N, 13.62; Found: C, 53.75; H, 5.53; N, 13.72. IR (KBr, ν cm^{-1}): 3148, 3126, 2976, 2934, 1609, 1583, 1496, 1449, 1382, 1288, 1097, 760, 704, 621. ^{1}HNMR (400MHz: CD_3CN, δppm, Figure. S3): 11.352 (s, 2H^5), 8.872 (s, 2H^4), 8.286 (s, 2H^3), 7.274 (t, J = 7.2 Hz, 4H^9), 7.185 (t, J = 7.2 Hz, 2H^{10}), 6.354 (d, J = 7.6 Hz, 4H^8), 3.908 (d, J = 14 Hz, 2H^6), 3.619 (t, J = 13 Hz, 4H^2), 2.203 (d, J = 34.8 Hz, 6H^7), 1.925 (m, 4H^1). ^{13}CNMR (400 MHz: CD_3CN, δppm, Figure. S4): 149.810, 143.677, 142.540, 140.228, 128.379, 126.891, 123.741, 117.010, 78.567, 47.721, 33.830, 27.406.

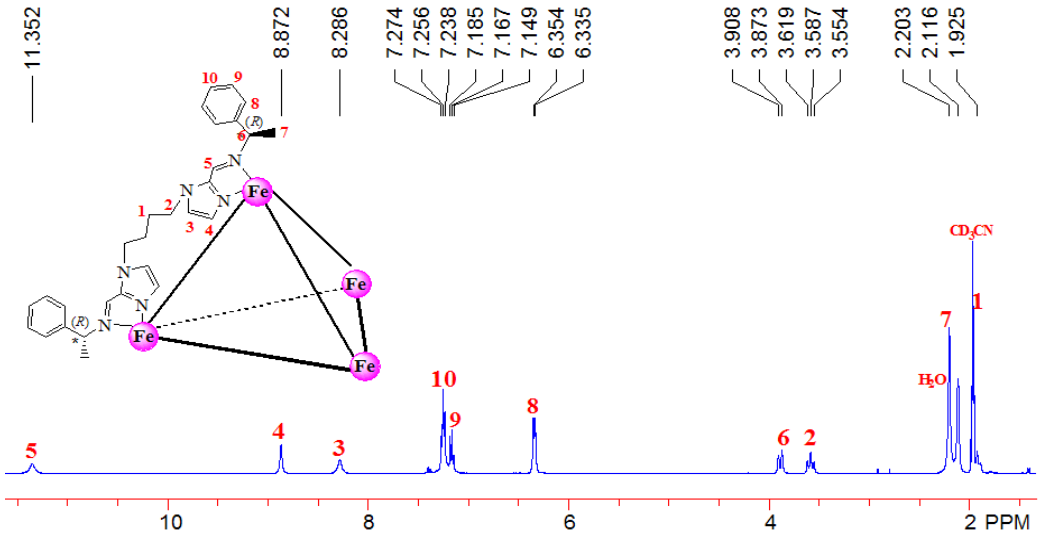

Fig. S3 ^{1}H NMR spectrum of cage **(*R*)-1**.

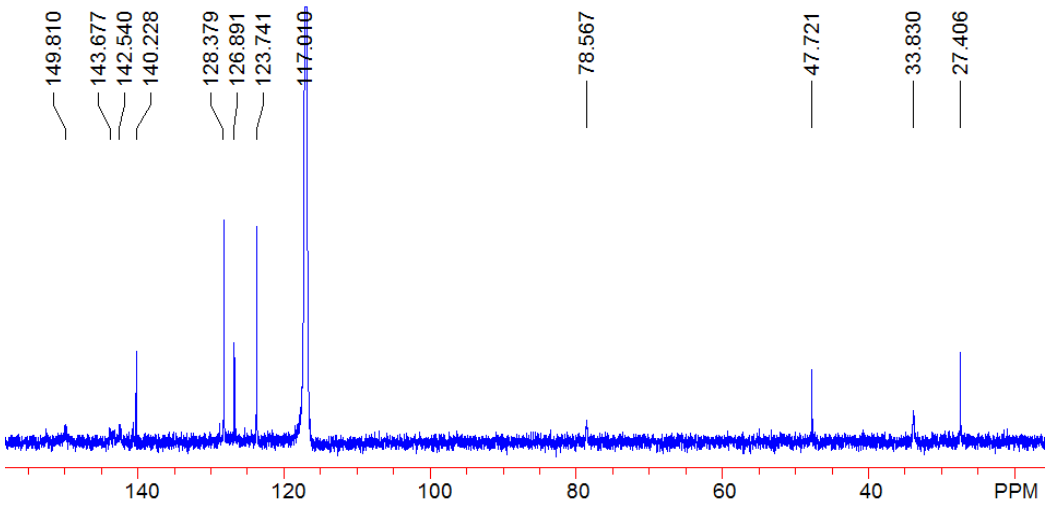

Fig. S4 ^{13}C NMR spectrum of cage **(*R*)-1**.

4. Synthesis of cage (*R*)-2 and (*S*)-2

These complexes were prepared by a similar procedure to that described for cage **1** except that (*R*)- or (*S*)-1-(4-methoxy-phenyl)ethylamine instead of (*R*)- or (*S*)-1-phenylethylamine was used. Purple crystals of cage **2** were obtained with 68% yield. Calcd for **(*R*)-2** $C_{180}H_{216}Cl_8Fe_4N_{36}O_{44}\cdot 2CH_3OCH_3\cdot 12CH_3CN\cdot H_2O$: C, 53.10; H, 5.59; N, 13.27; Found: C, 52.64; H, 5.37; N, 12.89. Calcd for **(*S*)-2** $C_{180}H_{216}Cl_8Fe_4N_{36}O_{44}\cdot Et_2O\cdot 6MeCN\cdot H_2O$: C, 53.10; H, 5.59; N, 13.27; Found: C, 52.78; H, 5.42; N, 12.93. IR (KBr, ν cm^{-1}): 3142, 3123, 2970, 2939, 1609, 1572, 1515, 1448, 1387, 1251, 1184, 1098, 840, 618. ^{1}HNMR (400MHz: CD_3CN, δppm, Figure. S5): 14.544 (s, 2H^5), 10.897 (s, 2H^4), 9.077 (s, 2H^3), 6.728 (t, J = 6.4 Hz, 4H^9), 6.130 (d, J = 5.2 Hz, 4H^8), 3.847 (d, J = 13.2 Hz, 2H^6), 3.736 (s, 2H^{10}), 3.493 (t, J = 10.8 Hz, 4H^2), 2.251 (d, J = 10.8 Hz, 6H^7), 1.921 (m, 4H^1). ^{13}CNMR (400 MHz: CD_3CN, δppm, Figure. S6): 158.480, 145.996, 138.303, 135.430, 132.447, 124.791, 117.003, 113.167, 84.655, 54.882, 48.195, 41.340, 27.026.

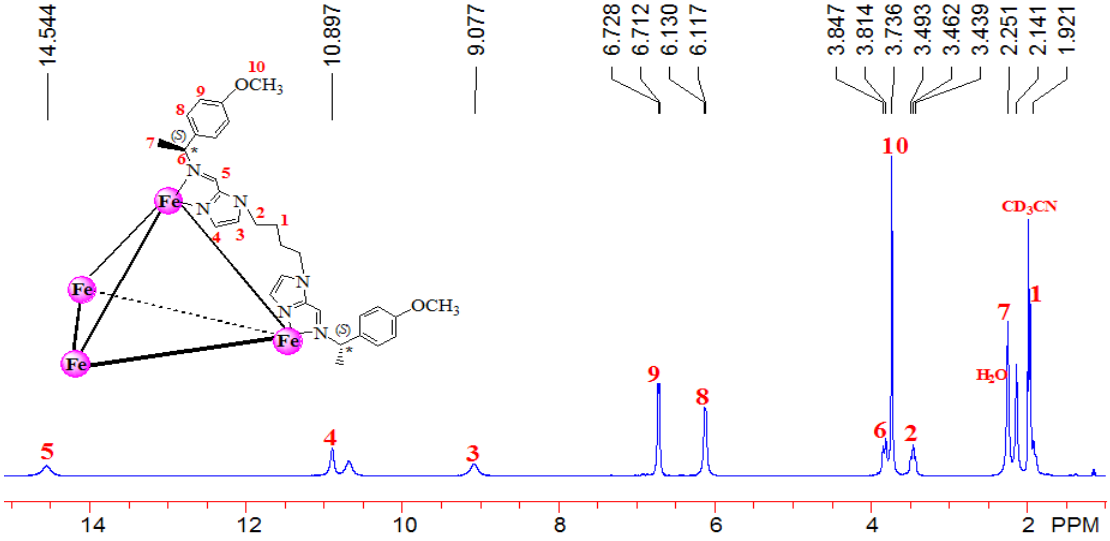

Fig. S5 ^{1}H NMR spectrum of cage **(*S*)-2**.

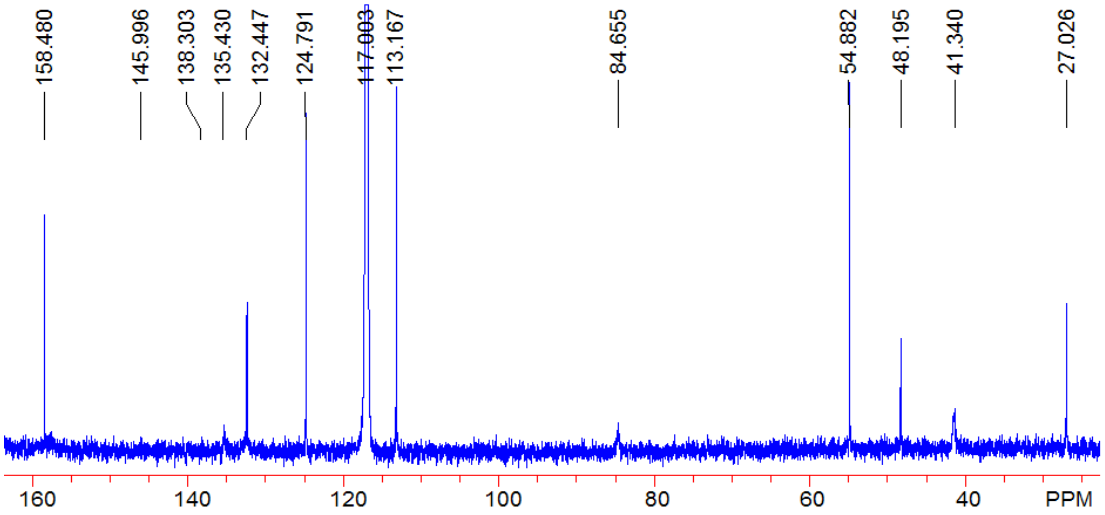

Fig. S6 ^{13}C NMR spectrum of cage **(*S*)-2**.

5. Synthesis of cage (*R*)-3 and (*S*)-3

These complexes were prepared by a similar procedure to that described for cage **1** except that (*R*)- or (*S*)-1-(4-chlorophenyl)ethylamine instead of (*R*)- or (*S*)-1-phenylethylamine was used. Purple crystals of cage **3** were obtained with 78% yield. Calcd for **(*S*)-3** $C_{168}H_{180}Cl_{20}Fe_4N_{36}O_{32}\cdot 2Et_2O\cdot 4MeCN\cdot H_2O$: C, 49.35; H, 4.82; N, 12.51; Found: C, 50.10; H, 4.61; N, 12.42. IR (KBr, ν cm^{-1}): 3152, 3124, 2973, 2931, 1608, 1570, 1495, 1449, 1378, 1285, 1094, 832, 775, 628. ^{1}HNMR (400MHz: CD_3CN, δppm, Figure. S7): 11.954 (s, 2H^{5}), 9.479 (s, 2H^{4}), 7.609 (s, 2H^{3}), 7.310 (t, J = 8 Hz, 4H^{9}), 6.286 (d, J = 7.6 Hz, 4H^{8}), 4.114 (d, J = 14 Hz, 2H^{6}), 3.762 (t, J = 13 Hz, 4H^{2}),

2.146 (d, J = 14.8 Hz, 6H^{7}), 1.955 (m, 4H^{1}). ^{13}CNMR (400 MHz: CD_3CN, δppm, Figure. S8): 151.195, 145.478, 141.410, 139.068, 132.447, 128.283, 125.454, 117.002, 78.507, 47.480, 34.274, 27.274.

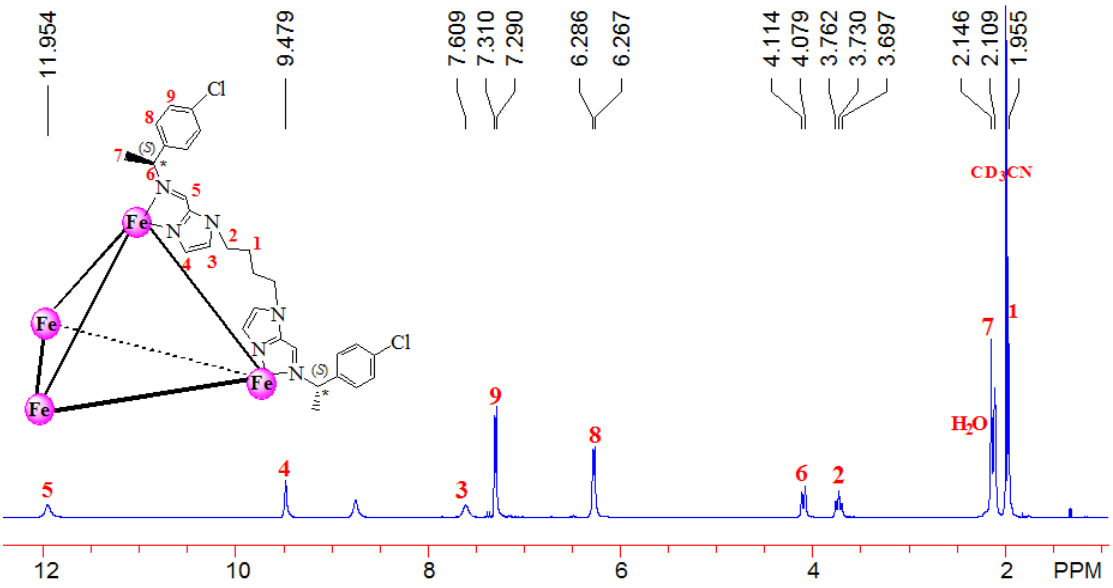

Fig. S7 ^{1}H NMR spectrum of cage **(*S*)-3**.

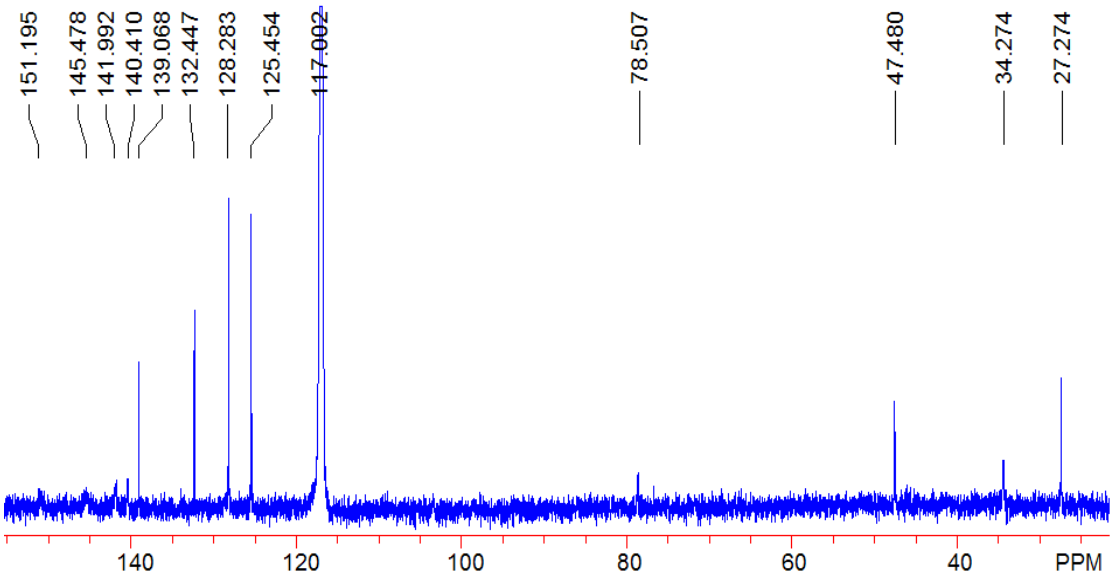

Fig. S8 ^{13}C NMR spectrum of cage **(*S*)-3**.

6. Additional structural figures

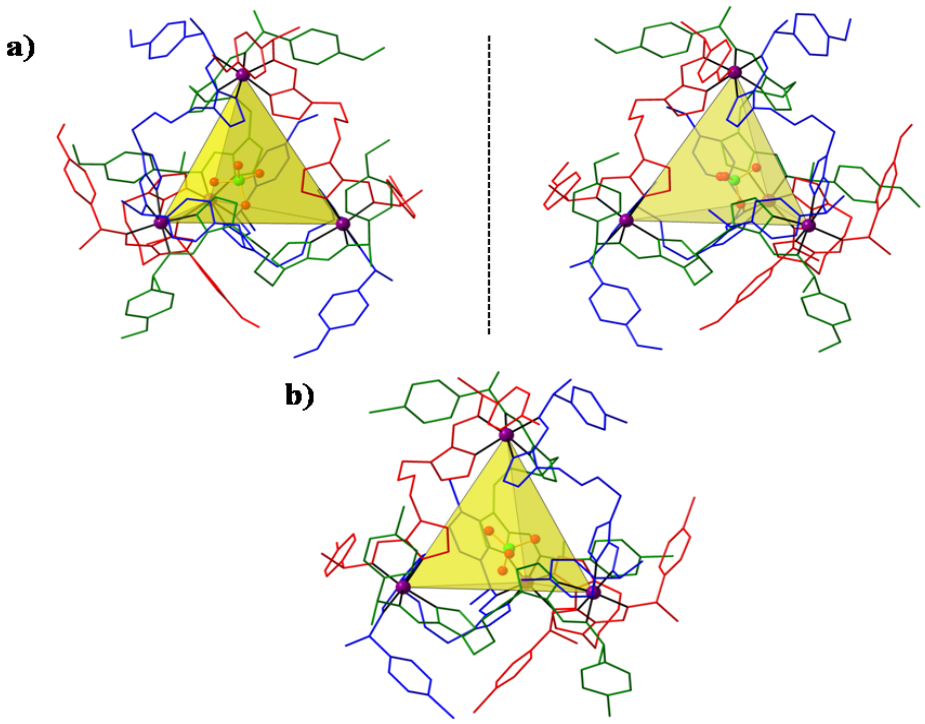

Fig. S9 X-ray crystal structures of a) enantiopure tetrahedral cages **(*R*)-2** (left) and **(*S*)-2** (right); b) cage **(*S*)-3**. All H atoms and the remaining seven anions have been removed for clarity.

7. CD and UV/Vis spectra

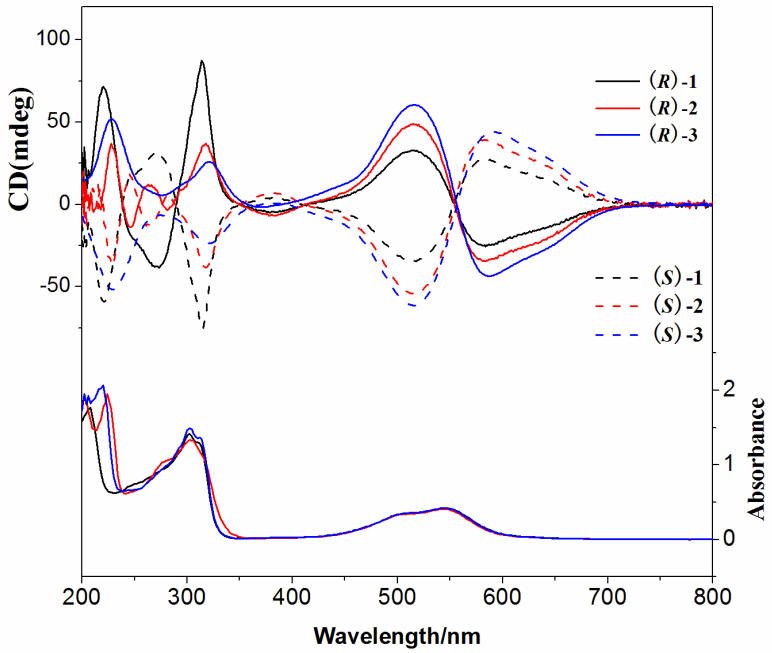

Fig. S10 CD (top) and UV/Vis (bottom) spectra of cages **1-3** in CH_3CN (20 μmol/L).

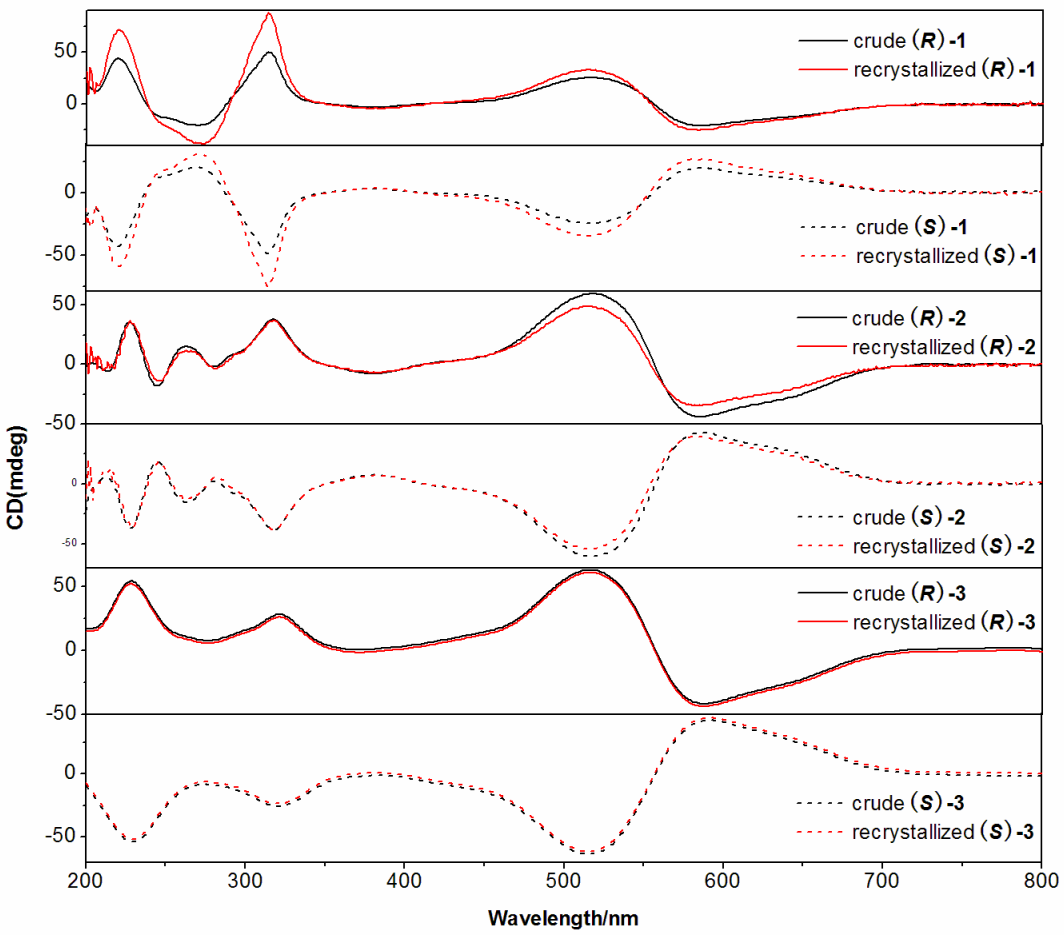

Fig. S11 CD spectra of crude and recrystallized cages **1-3** samples in CH_3CN (20 μmol/L).

8. Analysis of structure interconversion

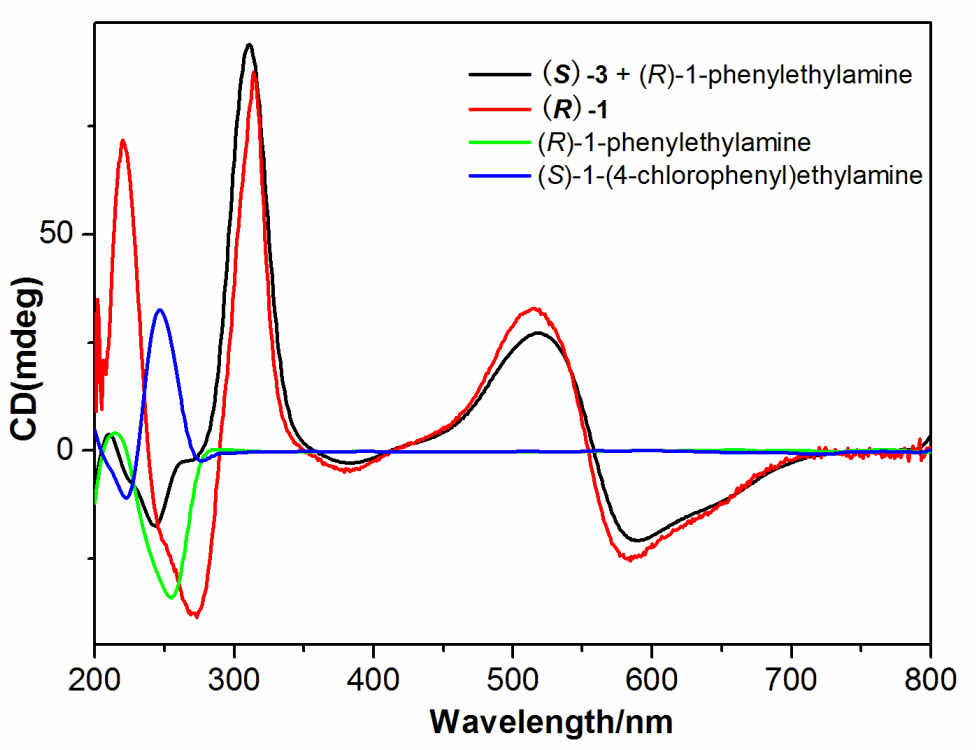

Fig. S12 CD spectra of transformation **(*S*)-3** to **(*R*)-1** in CH_3CN (20 μmol/L).

(*S*)-3→(*R*)-1: Into a test tube **(*S*)-3** (10.4 mg, 0.0025 mmol, 1 eq.), (*R*)-1-phenylethylamine (4.5 mg, 0.0375 mmol, 15 eq.) and CH_3CN (10 mL) were added. The tube was sealed and the solution was purified of dioxygen by nitrogen. The dark purple solution was placed at room temperature for two days. This transformation is complete with configuration inversion. Comparison with CD spectra of the sample obtained from self-assembly and transformation, the peaks in the range of 300-800 nm were almost identical, the peaks at 200-300 nm changed due to the excess (*R*)-1-phenylethylamine and (*S*)-1-(4-chlorophenyl)ethylamine.

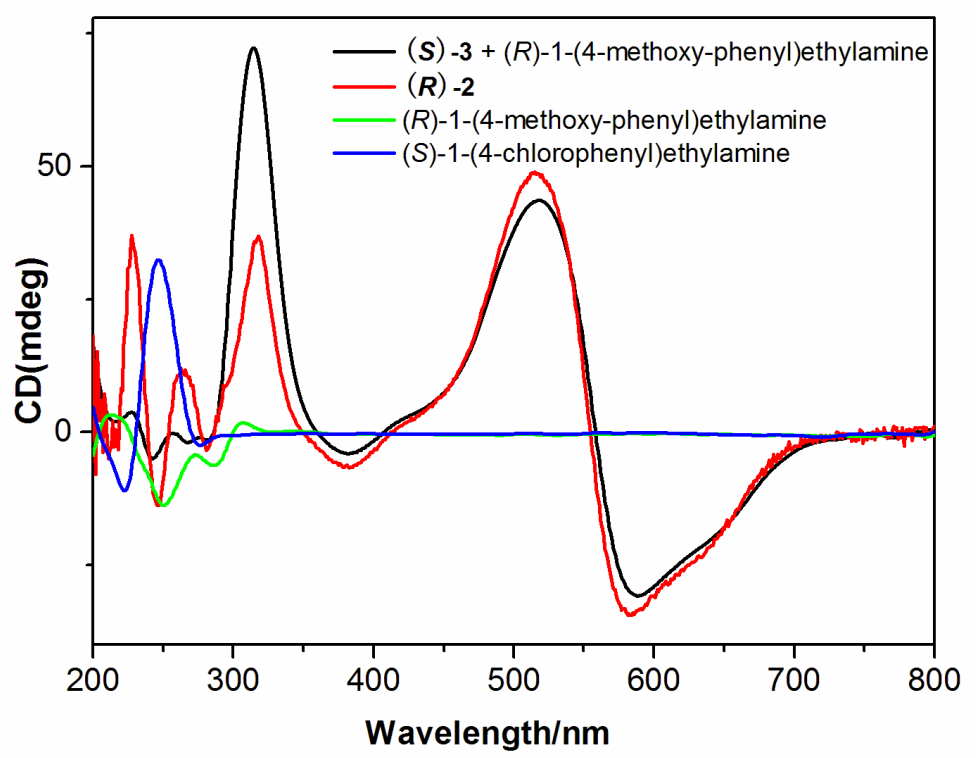

Fig. S13 CD spectra of transformation **(*S*)-3** to **(*R*)-2** in CH_3CN (20 μmol/L).

(*S*)-3→(*R*)-2: Into a test tube **(*S*)-3** (10.4 mg, 0.0025 mmol, 1 eq.), (*R*)-1-(4-methoxy-phenyl)ethylamine (5.7 mg, 0.0375 mmol, 15 eq.) and CH_3CN (10 mL) were added. The tube was sealed and the solution was purified of dioxygen by nitrogen. The dark purple solution was placed at room temperature for two days. This transformation is complete with configuration inversion. Comparison with CD spectra of the sample obtained from self-assembly and transformation, the peaks in the range of 300-800 nm were almost identical, the peaks at 200-300 nm changed due to the excess (*R*)-1-(4-methoxy-phenyl)ethylamine and (*S*)-1-(4-chlorophenyl)ethylamine.

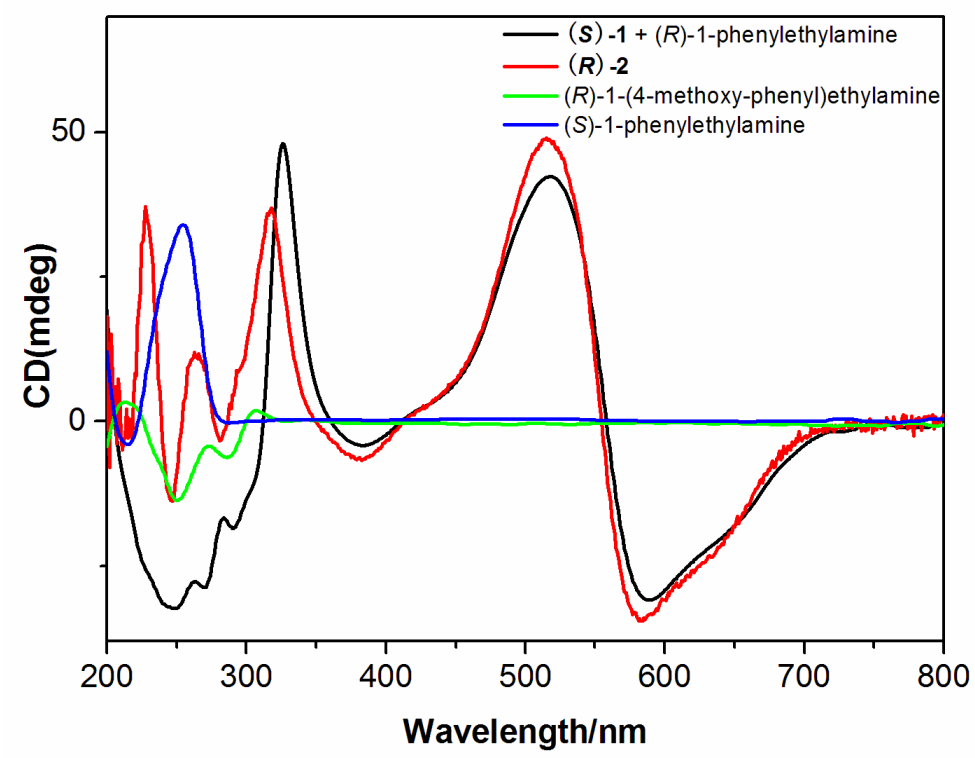

Fig. S14 CD spectra of transformation **(*S*)-1** to **(*R*)-2** in CH_3CN (20 μmol/L).

(*S*)-1→(*R*)-2: Into a test tube **(*S*)-1** (9.4 mg, 0.0025 mmol, 1 eq.), (*R*)-1-(4-methoxy-phenyl)ethylamine (5.7 mg, 0.0375 mmol, 15 eq.) and CH_3CN (10 mL) were added. The tube was sealed and the solution was purified of dioxygen by nitrogen. The dark purple solution was heated at 313 K for two days. This transformation is complete with configuration inversion. Comparison with CD spectra of the sample obtained from self-assembly and transformation, the peaks in the range of 300-800 nm were almost identical, the peaks at 200-300 nmchanged due to the excess (*R*)-1-(4-methoxy-phenyl)ethylamine and (*S*)-1-phenylethylamine.

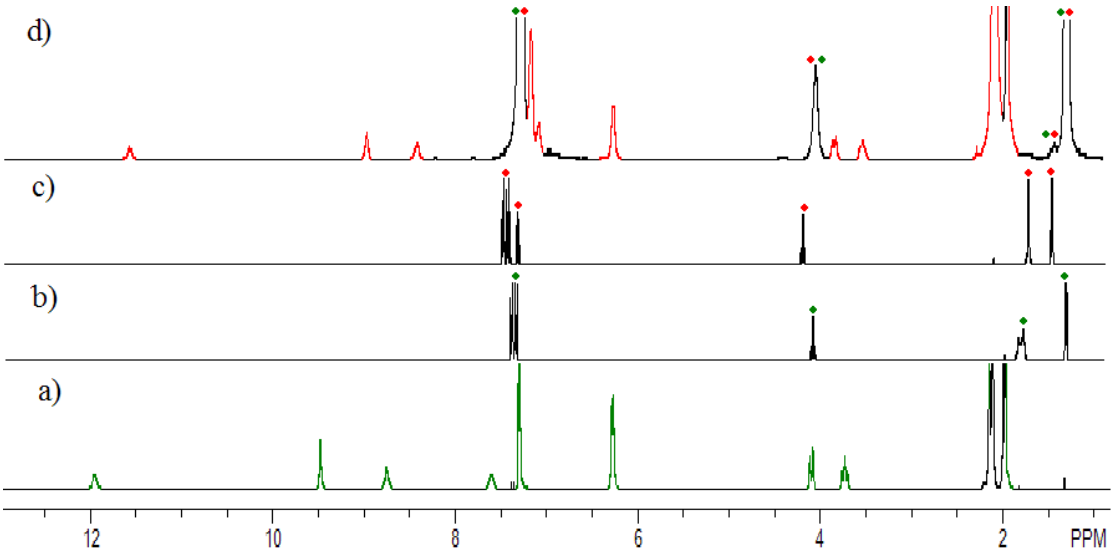

Fig. S15 ^{1}H NMR spectra: a) **(*S*)-3**; b) (*S*)-1-(4-chlorophenyl)ethylamine; c) (*S*)-1-phenylethylamine; d) **(*S*)-1** was formed through adding (*S*)-1-phenylethylamine into **(*S*)-3**. The signals from free subcomponents (*S*)-1-(4-chlorophenyl)ethylamine and (*S*)-1-phenylethylamine are marked by gree and red filled circles, respectively.

(*S*)-3→(*S*)-1: Into a NMR tube **(*S*)-3** (10.4 mg, 0.0025 mmol, 1 eq.), (*S*)-1-phenylethylamine (4.5 mg, 0.0375 mmol, 15 eq.) and CD_3CN (1 mL) were added. The tube was sealed and the solution was purified of dioxygen by nitrogen. The dark purple solution was placed at room temperature for two days. This transformation is complete, which is clearly observed by ^{1}H NMR (Figure S15): the peak at 11.954 ppm (imine protons) was observed to transform into a imine singlet at 11.467 ppm, peaks at 9.479 ppm, 7.609 ppm (imidazole protons) became at 8.835 ppm, 8.277 ppm, the two doublets between 6.267 and 7.310 ppm became two triplets and a doublet between 6.096 and 7.021 ppm, a doublet at 4.114 ppm,4.079 ppm became at 3.633 ppm, 3.666ppm, a triplet between 3.697 and 3.762 ppm became a triplet between 3.303 and 3.369 ppm.

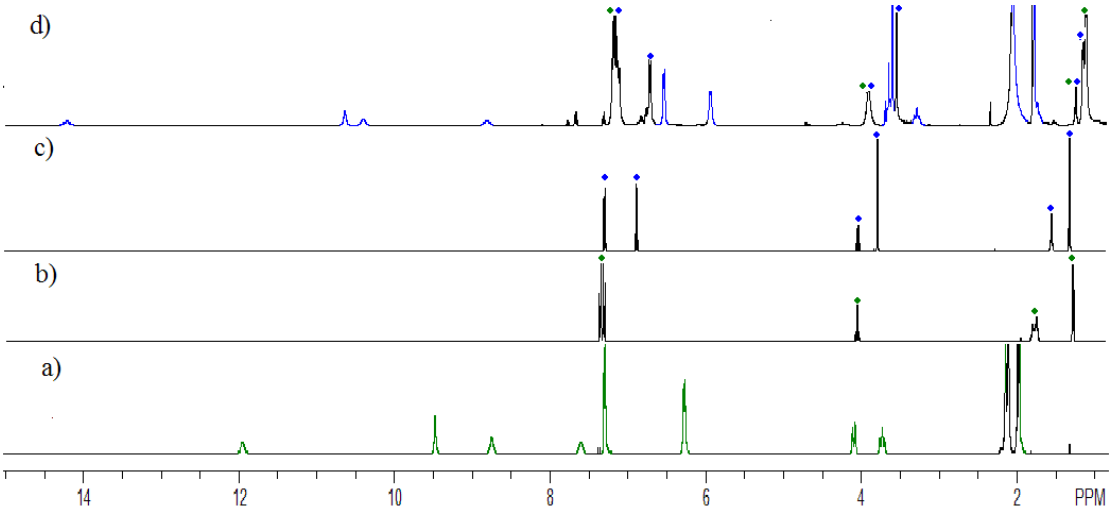

Fig. S16 ^{1}H NMR spectra: a) **(*S*)-3**; b) (*S*)-1-(4-chlorophenyl)ethylamine; c) (*S*)-1-(4-methoxy-phenyl)ethylamine; d) **(*S*)-2** was formed through adding (*S*)-1-(4-methoxy-phenyl)ethylamine into **(*S*)-3**. The signals from free subcomponents (*S*)-1-(4-chlorophenyl)ethylamine and (*S*)-1-(4-methoxy-phenyl)ethylamine are marked by gree and blue filled circles, respectively.

(*S*)-3→(*S*)-2: Into a NMR tube **(*S*)-3** (10.4 mg, 0.0025 mmol, 1 eq.), (*S*)-1-(4-methoxy-phenyl)ethylamine (5.7 mg, 0.0375 mmol, 15 eq.) and CD_3CN (1 mL) were added. The tube was sealed and the solution was purified of dioxygen by nitrogen. The dark purple solution was placed at room temperature for two days. This transformation is complete, which is clearly observed by ^{1}H NMR (Figure S16): the peak at 11.954 ppm (imine protons) was observed to transform into a imine singlet at 14.176 ppm, peaks at 9.479 ppm, 7.609 ppm (imidazole protons) became at 10.600 ppm, 8.779 ppm, the two doublets between 6.267 and 7.310 ppm became two doublets between 5.893 and 6.509 ppm, a doublet at 4.114 ppm,4.079 ppm and a triplet between 3.697 and 3.762 ppm became a double at 3.612 ppm, 3.656ppm, a triplet between 3.215 and 3.282 ppm and a sharp singlet at 3.585 ppm. The several small peaks observed belong to unknown new species.

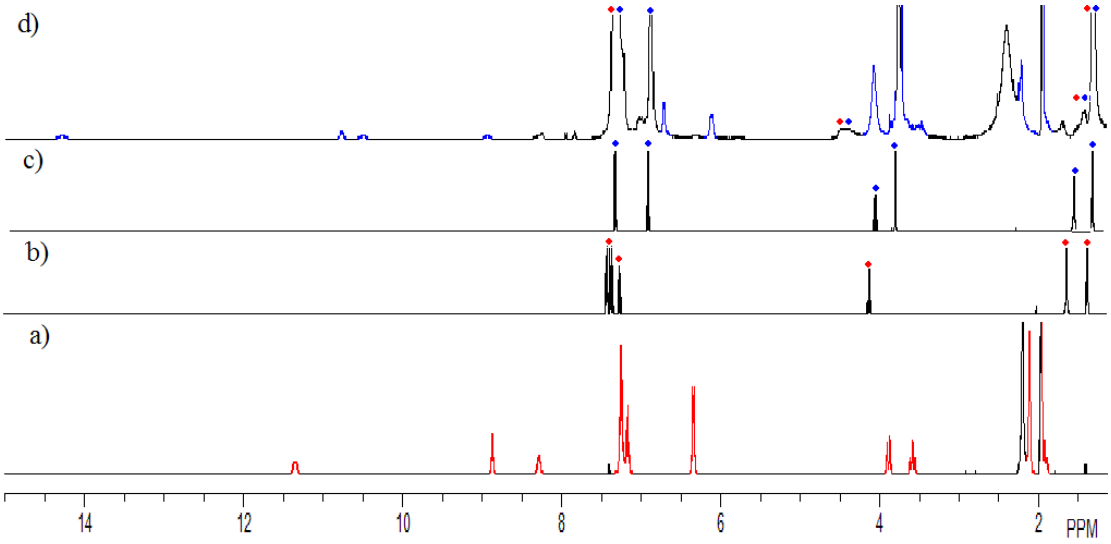

Fig. S17 ^{1}H NMR spectra: a) **(*S*)-1**; b) (*S*)-1-phenylethylamine; c) (*S*)-1-(4-methoxy-phenyl)ethylamine; d) **(*S*)-2** was formed through adding (*S*)-1-(4-methoxy-phenyl)ethylamine into **(*S*)-1**. The signals from free subcomponents (*S*)-1-phenylethylamine and (*S*)-1-(4-methoxy-phenyl)ethylamine are marked by red and blue filled circles, respectively.

(*S*)-1→(*S*)-2: Into a NMR tube **(*S*)-1** (9.4 mg, 0.0025 mmol, 1 eq.), (*S*)-1-(4-methoxy-phenyl)ethylamine (5.7 mg, 0.0375 mmol, 15 eq.) and CD_3CN (1 mL) were added. The tube was sealed and the solution was purified of dioxygen by nitrogen. The dark purple solution was heated at 313 K for one day. This transformation is complete, which is clearly observed by ^{1}H NMR (Figure S17): the peak at 11.352ppm (imine protons) was observed to transform into a imine singlet at 14.275 ppm, peaks at 8.872 ppm, 8.286 ppm (imidazole protons) became at 10.766 ppm, 8.936 ppm, two triplets and a doublet between 6.335 and 7.274 ppm became two doublets between 6.100 and 6.709 ppm, a doublet at 3.873 ppm,3.908 ppm and a triplet between 3.554 and 3.619 ppm became a double at 3.804 ppm, 3.853ppm, a triplet between 3.426 and 3.489 ppm and a sharp singlet at 3.758 ppm. The several small peaks observed belong to unknown new species.

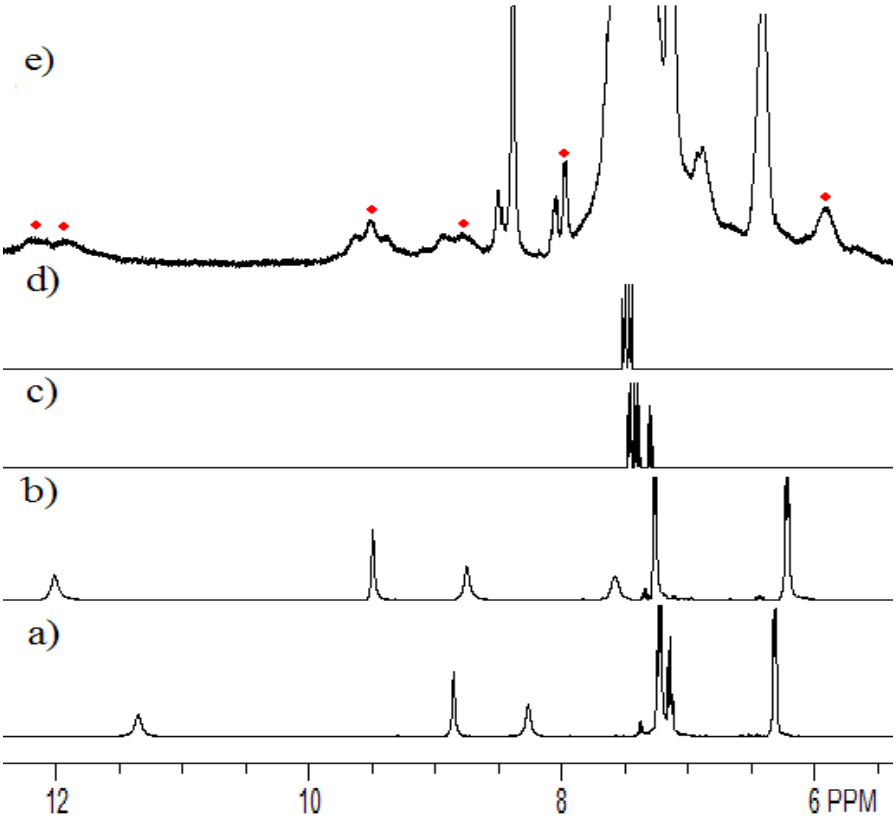

Fig. S18 ^{1}H NMR spectra: a) **(*S*)-1**; b) **(*S*)-3**; c) (*S*)-1-phenylethylamine; d) (*S*)-1-(4-chlorophenyl)ethylamine; e) part of **(*S*)-1** convert into **(*S*)-3** through adding (*S*)-1-(4-chlorophenyl)ethylamine into **(*S*)-1**. The signals from new species are marked by red filled circles.

Into a NMR tube **(*S*)-1** (9.4 mg, 0.0025 mmol, 1 eq.), (*S*)-1-(4-chlorophenyl)ethylamine (7.6 mg, 0.0500 mmol, 20 eq.) and CD_3CN (1 mL) were added. The tube was sealed and the solution was purified of dioxygen by nitrogen. The dark purple solution was heated at 313 K for two days. This transformation is incomplete, which is clearly observed by ^{1}H NMR (Figure S18): new peaks were found in spectra belong to new species, which are marked by red filled circles.

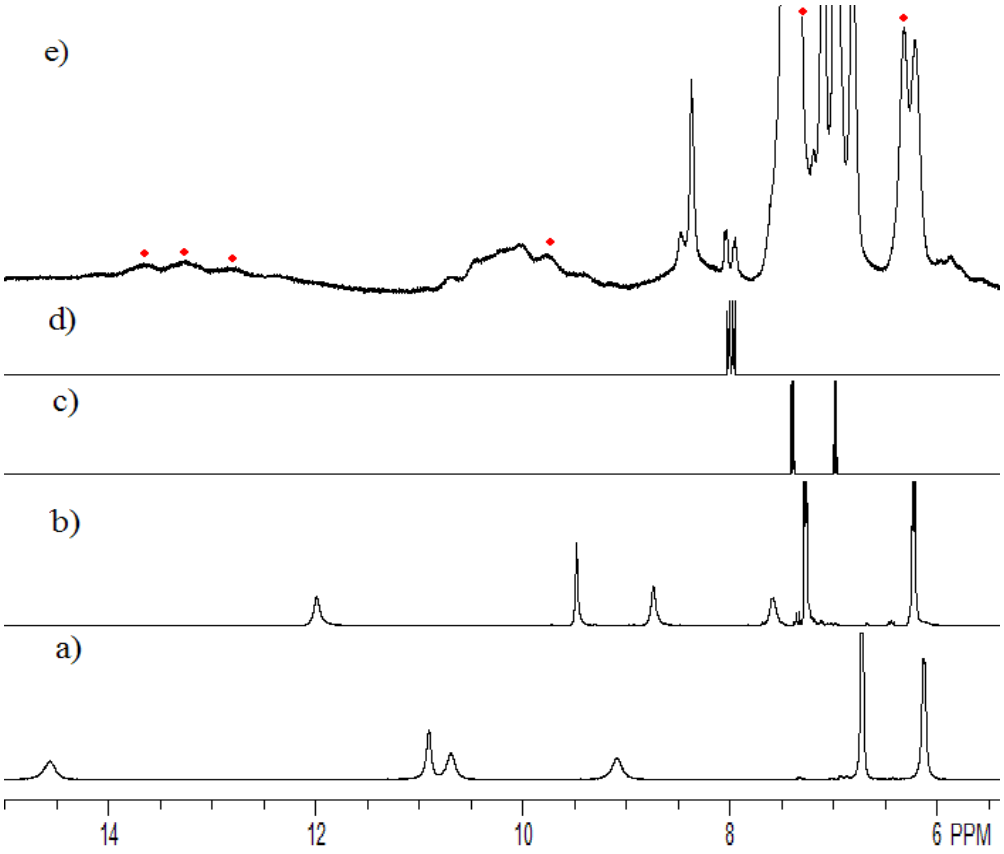

Fig. S19 ^{1}H NMR spectra: a) **(*S*)-2**; b) **(*S*)-3**; c) (*S*)-1-(4-methoxy-phenyl)ethylamine; d) (*S*)-1-(4-chlorophenyl)ethylamine; e) part of **(*S*)-2** conwetr into **(*S*)-3** through adding (*S*)-1-(4-chlorophenyl)ethylamine into **(*S*)-2**. The signals from new species are marked by red filled circles.

Into a NMR tube **(*S*)-2** (10.3 mg, 0.0025 mmol, 1 eq.), (*S*)-1-(4-chlorophenyl)ethylamine (7.6 mg, 0.0500 mmol, 20 eq.) and CD_3CN (1 mL) were added. The tube was sealed and the solution was purified of dioxygen by nitrogen. The dark purple solution was heated at 313 K for two days. This transformation is incomplete, which is clearly observed by ^{1}H NMR (Figure S19): new peaks were found in spectra belong to new species, which are marked by red filled circles.

9. Analysis of TG spectra

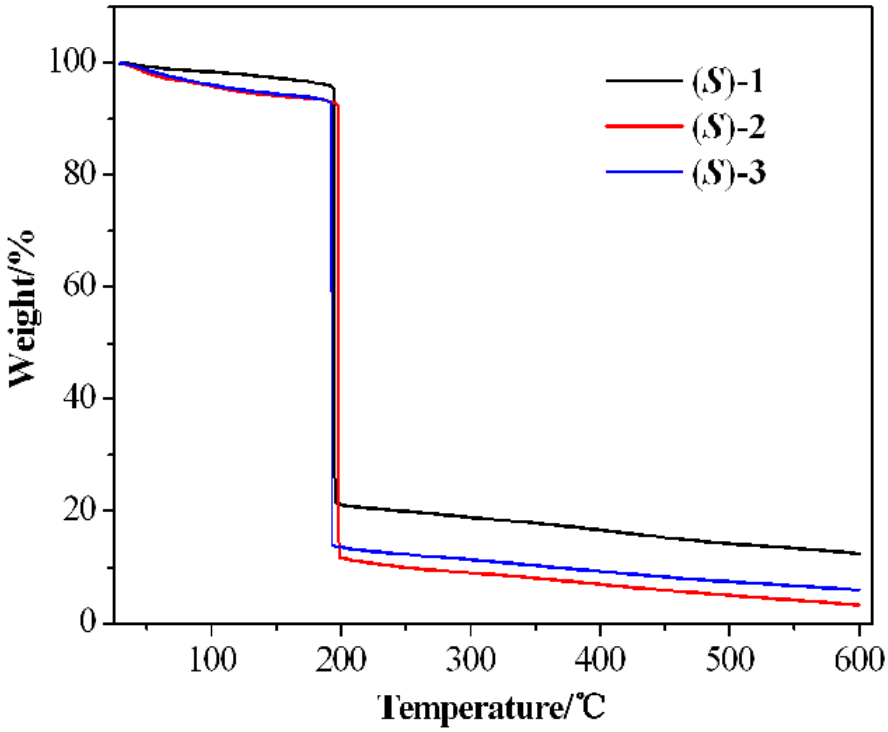

Fig. S20 Thermogravimetric analysis for cages **(*S*)-1, (*S*)-2, (*S*)-3**.

In three lines the first weigh loss until 195 °C, 197 °C, and 191 °C, was due to the uncoordinated 1 Et_2O, 2 MeCN and 1 H_2O for ***S*-1**, 1 Et_2O, 6 MeCN and 2 H_2O for ***S*-2**, 2 Et_2O, 4 MeCN and 1 H_2O for ***S*-3** (obsd 4.54%, 7.59%, 7.18%, respectively). The decomposition of the organic links in the anhydrous compounds occur at 195-600 °C, 197-600 °C, and 191-600 °C, respectively. The remaining weights correspond to the formation of Fe_xO_y, (obsd 12.55%, 3.28%, 5.90% respectively).

10. X-ray Crystallography

The crystal structures were determined on a Siemens (Bruker) SMART CCD

diffractometer using monochromated Mo $K\alpha$ radiation (λ = 0.71073 Å) at 150 or 123 K. Cell parameters were retrieved using SMART software and refined using SAINT[1] on all observed reflections. The highly redundant data sets were reduced using SAINT[1] and corrected for Lorentz and polarization effects. Absorption corrections were applied using SADABS[2] supplied by Bruker. Structures were solved by direct methods using the program SHELXL-97.[3] All of the non-hydrogen atoms except the disordered solvent molecules and anions were refined with anisotropic thermal displacement coefficients. Hydrogen atoms of organic ligands were located geometrically and refined in a riding model, whereas those of solvent molecules were not treated during the structural refinements. Disorder was modelled using standard crystallographic methods including constraints, restraints and rigid bodies where necessary. For compound **1*R***, the oxygen atoms O(5), O(6), O(7) and O(8) bound to Cl(2) and O(11) and O(12) bound to Cl(4) for perchlorate anions are disordered. For compound **1*S***, the oxygen atoms O(3) and O(4) bound to Cl(2) for perchlorate anion are disordered. For compound **2*R***, one 1-(4-methoxy-phenyl)ethylamine group (C82-C90 and O6) is disordered, two perchlorate ions (Cl(4) and Cl(8)) are disordered, and the oxygen atoms bound to Cl(5) and Cl(6) are disordered. For compound **2*S***, two 1-(4-methoxy-phenyl)ethylamine groups (C82-C90, O6, C242-C250 and O10) are disordered, and two perchlorate ions (Cl(7) and Cl(8)) are disordered. For compound **3*S***, one 1-(4-chlorophenyl)ethylamine group (C9-C16 and Cl1) is disordered, and one perchlorate ion (Cl(8)) is disordered. The crystals of **1-3** decayed rapidly out of solvent. Despite rapid handling and long exposure times, the data collected are less than ideal quality. Nevertheless, the data for **1-3** are of more than sufficient quality to unambiguously establish the connectivity of the structures. Reflecting the instability of the crystals, there is a large area of smeared electron density present in the lattice. Despite many attempts to model this region of disorder as a combination of solvent molecules no reasonable fit could be found and accordingly this region was treated with the SQUEEZE function of PLATON. Final crystallographic data and values of R_1 and wR for **1**–**4** are listed in Tables S1-S2. Selected bond distances and angles are

given in Table S3.

Table S1. Crystallographic data for cages **(*R*)-1** and **(*S*)-1**.

	(*R*)-1	**(*S*)-1**
formula	$C_{168}H_{192}C_{l8}Fe_4N_{36}O_{32}$	$C_{168}H_{192}C_{l8}Fe_4N_{36}O_{32}$
fw	3734.58	3734.58
T (K)	150(2)	123(2)
λ (Å)	0.71073	0.71073
crystal system	Trigonal	Trigonal
space group	*R*3	*R*3
a (Å)	30.682(4)	30.825(8)
b (Å)	30.682(4)	30.825(8)
c (Å)	23.596(5)	22.939(11)
α (^{0})	90	90
β (^{0})	90	90
γ (^{0})	120	120
V (Å^3)	19237(5) Å^3	18877(12)
Z	3	3
D_{calc} (Mg/m^3)	0.967	0.986
μ (mm^{-1})	0.362	0.368
F(000)	5844	5844
θ (^{0})	3.26-25.49	3.18-25.05
index ranges	-32 ≤ h ≤ 30,	-29 ≤ h ≤ 36,
	-27 ≤ k ≤ 37,	-36 ≤ k ≤ 31,
	-23 ≤ l ≤ 28	-25 ≤ l ≤ 9
reflections collected	14892	7838
GOF (F^2)	1.008	1.287
Flack χ	0.06(3)	0.12(6)
$R_1{}^a$, $wR_2{}^b$ (I>2σ(I))	0.1042, 0.2759	0.1395, 0.3552
$R_1{}^a$, $wR_2{}^b$ (all data)	0.1389, 0.3113	0.1690, 0.3745

$R_1{}^a = \Sigma||F_o| - |F_c||/\Sigma F_o|$. $wR_2{}^b = [\Sigma w(F_o{}^2 - F_c{}^2)^2/\Sigma w(F_o{}^2)]^{1/2}$

Table S2. Crystallographic data for cages **(*R*)-2, (*S*)-2** and **(*S*)-3**.

	(*R*)-2	**(*S*)-2**	**(*S*)-3**
formula	$C_{211.17}H_{272.75}C_{l8}Fe_4N_{47.58}O_{47}$	$C_{192}H_{234}C_{l8}Fe_4N_{42}O_{44}$	$C_{174}H_{189}C_{l20}Fe_4N_{39}O_{32}$
fw	4736.68	4341.21	4271.04

T (K)	123(2)	123(2)	123(2)
λ (Å)	0.71073	0.71073	0.71073
crystal system	Triclinic	Triclinic	Trigonal
space group	$P\bar{1}$	$P\bar{1}$	$R\bar{3}$
a (Å)	19.6065(9)	19.7723(13)	31.4702(14)
b (Å)	19.7357(8)	19.7731(14)	31.4702(14)
c (Å)	20.2252(9)	20.282(2)	22.296(2)
α (^{0})	116.6207(11)	115.476(2)	90
β (^{0})	115.5608(12)	116.397(2)	90
γ (^{0})	94.4565(13)	94.9610(10)	120
V (Å^3)	5944.6(5)	6022.1(9)	19123(2)
Z	1	1	3
D_{calc} (Mg/m^3)	1.323	1.197	1.113
μ (mm^{-1})	0.411	0.398	0.493
F(000)	2489	2272	6618
θ (^{0})	2.99-25.08	1.22-25.50	1.18-26.47
index ranges	-23 ≤ h ≤ 23,	-23 ≤ h ≤ 23,	-36 ≤ h ≤ 37,
	-23 ≤ k ≤ 23,	-23 ≤ k ≤ 23,	-38 ≤ k ≤ 39,
	-24 ≤ l ≤ 21	-24 ≤ l ≤ 21	-27 ≤ l ≤ 9
reflections collected	51620	50101	21930
GOF (F^2)	1.061	0.963	0.935
Flack χ	-0.036(17)	0.004(14)	0.10(4)
$R_1{}^a$, $wR_2{}^b$ (I>2σ(I))	0.0832, 0.2055	0.0758, 0.1914	0.0639, 0.1665
$R_1{}^a$, $wR_2{}^b$ (all data)	0.1278, 0.2337	0.1315, 0.2181	0.0943, 0.1805

$R_1{}^a = \Sigma||F_o| - |F_c||/\Sigma F_o|$. $wR_2{}^b = [\Sigma w(F_o{}^2 - F_c{}^2)^2/\Sigma w(F_o{}^2)]^{1/2}$

Table S3. Selected bond lengths [Å] and angles [°] for cages **(*R*)-1, (*S*)-1**, **(*R*)-2, (*S*)-2** and **(*S*)-3**.

cage (*R*)-1			
Fe(1)-N(11)#5	1.936(8)	Fe(2)-N(5)#6	1.931(7)
Fe(1)-N(2)	1.951(8)	Fe(2)-N(5)	1.931(7)
Fe(1)-N(8)	1.965(8)	Fe(2)-N(5)#5	1.931(7)
Fe(1)-N(9)	1.991(7)	Fe(2)-N(6)	2.004(8)
Fe(1)-N(3)	2.001(9)	Fe(2)-N(6)#6	2.005(8)
Fe(1)-N(12)#5	2.033(8)	Fe(2)-N(6)#5	2.005(8)
N(11)#5-Fe(1)-N(2)	92.6(4)	N(5)#6-Fe(2)-N(5)	91.6(3)
N(11)#5-Fe(1)-N(8)	92.3(4)	N(5)#6-Fe(2)-N(5)#5	91.6(3)
N(2)-Fe(1)-N(8)	92.4(4)	N(5)-Fe(2)-N(5)#5	91.6(3)

N(11)#5-Fe(1)-N(9)	169.8(4)	N(5)#6-Fe(2)-N(6)	92.3(3)
N(2)-Fe(1)-N(9)	94.2(3)	N(5)-Fe(2)-N(6)	82.0(3)
N(8)-Fe(1)-N(9)	79.9(4)	N(5)#5-Fe(2)-N(6)	172.6(3)
N(11)#5-Fe(1)-N(3)	91.3(4)	N(5)#6-Fe(2)-N(6)#6	82.0(3)
N(2)-Fe(1)-N(3)	82.1(4)	N(5)-Fe(2)-N(6)#6	172.6(3)
N(8)-Fe(1)-N(3)	173.5(4)	N(5)#5-Fe(2)-N(6)#6	92.3(3)
N(9)-Fe(1)-N(3)	97.1(4)	N(6)-Fe(2)-N(6)#6	94.5(3)
N(11)#5-Fe(1)-N(12)#5	78.3(4)	N(5)#6-Fe(2)-N(6)#5	172.6(3)
N(2)-Fe(1)-N(12)#5	169.3(4)	N(5)-Fe(2)-N(6)#5	92.3(3)
N(8)-Fe(1)-N(12)#5	93.5(4)	N(5)-Fe(2)-N(6)#5	82.0(3)
N(9)-Fe(1)-N(12)#5	95.6(4)	N(6)-Fe(2)-N(6)#5	94.5(3)
N(3)-Fe(1)-N(12)#5	92.5(3)	N(6)-Fe(2)-N(6)#6	94.5(3)
		cage (*S*)-1	
Fe(1)-N(8)	1.921(13)	Fe(2)-N(11)#1	1.917(12)
Fe(1)-N(5)#2	1.951(11)	Fe(2)-N(11)#2	1.917(12)
Fe(1)-N(6)#2	2.009(14)	Fe(2)-N(11)	1.917(12)
Fe(1)-N(9)	2.017(13)	Fe(2)-N(12)	2.013(15)
Fe(1)-N(3)	2.06(2)	Fe(2)-N(12)#2	2.013(15)
N(6)-Fe(1)#1	2.009(14)	Fe(2)-N(12)#1	2.013(15)
N(2)-Fe(1)-N(8)	91.3(5)	N(11)#1-Fe(2)-N(11)#2	92.5(5)
N(2)-Fe(1)-N(5)#2	90.7(5)	N(11)#1-Fe(2)-N(11)	92.5(5)
N(8)-Fe(1)-N(5)#2	90.0(6)	N(11)#2-Fe(2)-N(11)	92.5(5)
N(2)-Fe(1)-N(6)#2	168.9(6)	N(11)#1-Fe(2)-N(12)	173.5(5)
N(8)-Fe(1)-N(6)#2	93.4(6)	N(11)#2-Fe(2)-N(12)	92.6(6)
N(5)#2-Fe(1)-N(6)#2	79.3(5)	N(11)-Fe(2)-N(12)	83.2(5)
N(2)-Fe(1)-N(9)	92.6(5)	N(11)#1-Fe(2)-N(12)#2	92.6(6)
N(8)-Fe(1)-N(9)	80.3(5)	N(11)#2-Fe(2)-N(12)#2	83.2(5)
N(5)#2-Fe(1)-N(9)	169.9(6)	N(11)-Fe(2)-N(12)#2	173.5(5)
N(6)#2-Fe(1)-N(9)	98.1(5)	N(12)-Fe(2)-N(12)#2	92.0(7)
N(2)-Fe(1)-N(3)	80.8(5)	N(11)#1-Fe(2)-N(12)#1	83.2(5)
N(8)-Fe(1)-N(3)	172.1(6)	N(11)#2-Fe(2)-N(12)#1	173.5(5)
N(5) #2-Fe(1)-N(3)	91.1(6)	N(11)-Fe(2)-N(12)#1	92.6(6)
N(6) #2-Fe(1)-N(3)	94.6(6)	N(12)-Fe(2)-N(12)#1	92.0(7)
N(9)-Fe(1)-N(3)	98.9(6)	N(12)#2-Fe(2)-N(12)#1	92.0(7)
		cage (*R*)-2	
Fe(1)-N(2)	1.947(7)	Fe(3)-N(11)	1.932(7)
Fe(1)-N(14)	1.963(7)	Fe(3)-N(23)	1.939(8)
Fe(1)-N(8)	1.963(7)	Fe(3)-N(32)	1.953(7)

Fe(1)-N(15)	1.993(7)	Fe(3)-N(12)	1.978(8)
Fe(1)-N(3)	2.010(7)	Fe(3)-N(33)	1.998(8)
Fe(1)-N(9)	2.018(7)	Fe(3)-N(24)	2.009(8)
Fe(2)-N(20)	1.936(7)	Fe(4)-N(35)	1.940(7)
Fe(2)-N(26)	1.949(7)	Fe(4)-N(17)	1.950(7)
Fe(2)-N(5)	1.958(6)	Fe(4)-N(29)	1.965(7)
Fe(2)-N(21)	1.994(6)	Fe(4)-N(36)	1.997(8)
Fe(2)-N(27)	2.020(7)	Fe(4)-N(30)	2.024(8)
Fe(2)-N(6)	2.032(7)	Fe(4)-N(18)	2.039(8)
N(2)-Fe(1)-N(14)	92.8(3)	N(11)-Fe(3)-N(23)	92.1(3)
N(2)-Fe(1)-N(8)	90.8(3)	N(11)-Fe(3)-N(32)	90.5(3)
N(14)-Fe(1)-N(8)	91.2(3)	N(23)-Fe(3)-N(32)	90.8(3)
N(2)-Fe(1)-N(15)	172.7(3)	N(11)-Fe(3)-N(12)	80.5(3)
N(14)-Fe(1)-N(15)	80.6(3)	N(23)-Fe(3)-N(12)	172.3(3)
N(8)-Fe(1)-N(15)	92.5(3)	N(32)-Fe(3)-N(12)	91.6(3)
N(2)-Fe(1)-N(3)	81.4(3)	N(11)-Fe(3)-N(33)	171.4(3)
N(14)-Fe(1)-N(3)	91.6(3)	N(23)-Fe(3)-N(33)	90.8(3)
N(8)-Fe(1)-N(3)	171.8(3)	N(32)-Fe(3)-N(33)	81.3(3)
N(15)-Fe(1)-N(3)	95.5(3)	N(12)-Fe(3)-N(33)	96.9(3)
N(2)-Fe(1)-N(9)	92.9(3)	N(11)-Fe(3)-N(24)	94.1(3)
N(14)-Fe(1)-N(9)	170.2(3)	N(23)-Fe(3)-N(24)	80.8(3)
N(8)-Fe(1)-N(9)	80.8(3)	N(32)-Fe(3)-N(24)	170.6(3)
N(15)-Fe(1)-N(9)	94.1(3)	N(12)-Fe(3)-N(24)	97.3(3)
N(3)-Fe(1)-N(9)	97.1(3)	N(33)-Fe(3)-N(24)	94.4(3)
N(20)-Fe(2)-N(26)	90.9(3)	N(35)-Fe(4)-N(17)	88.3(3)
N(20)-Fe(2)-N(5)	90.7(3)	N(35)-Fe(4)-N(29)	88.9(3)
N(26)-Fe(2)-N(5)	88.8(3)	N(17)-Fe(4)-N(29)	89.9(3)
N(20)-Fe(2)-N(21)	81.1(3)	N(35)-Fe(4)-N(36)	80.9(3)
N(26)-Fe(2)-N(21)	92.5(3)	N(17)-Fe(4)-N(36)	93.8(3)
N(5)-Fe(2)-N(21)	171.7(3)	N(29)-Fe(4)-N(36)	169.0(3)
N(20)-Fe(2)-N(27)	171.4(3)	N(35)-Fe(4)-N(30)	93.0(3)
N(26)-Fe(2)-N(27)	80.7(3)	N(17)-Fe(4)-N(30)	170.3(3)
N(5)-Fe(2)-N(27)	91.0(3)	N(29)-Fe(4)-N(30)	80.5(3)
N(21)-Fe(2)-N(27)	97.3(3)	N(36)-Fe(4)-N(30)	95.9(3)
N(20)-Fe(2)-N(6)	92.3(3)	N(35)-Fe(4)-N(18)	167.9(3)
N(26)-Fe(2)-N(6)	169.2(3)	N(17)-Fe(4)-N(18)	80.2(3)
N(5)-Fe(2)-N(6)	80.8(3)	N(29)-Fe(4)-N(18)	94.8(3)
N(21)-Fe(2)-N(6)	98.1(3)	N(36)-Fe(4)-N(18)	96.0(3)

N(27)-Fe(2)-N(6)	96.2(3)	N(30)-Fe(4)-N(18)	99.0(3)
		cage (*S*)-2	
Fe(1)-N(8)	1.938(6)	Fe(3)-N(23)	1.935(6)
Fe(1)-N(2)	1.944(6)	Fe(3)-N(32)	1.936(6)
Fe(1)-N(14)	1.961(6)	Fe(3)-N(11)	1.953(6)
Fe(1)-N(3)	1.996(6)	Fe(3)-N(24)	1.993(5)
Fe(1)-N(15)	1.997(6)	Fe(3)-N(12)	2.005(6)
Fe(1)-N(9)	2.005(6)	Fe(3)-N(33)	2.015(6)
Fe(2)-N(5)	1.922(6)	Fe(4)-N(17)	1.927(6)
Fe(2)-N(20)	1.933(6)	Fe(4)-N(29)	1.931(5)
Fe(2)-N(26)	1.954(5)	Fe(4)-N(35)	1.932(6)
Fe(2)-N(6)	1.969(6)	Fe(4)-N(36)	2.000(7)
Fe(2)-N(21)	2.006(6)	Fe(4)-N(30)	2.002(7)
Fe(2)-N(27)	2.027(6)	Fe(4)-N(18)	2.025(6)
N(8)-Fe(1)-N(2)	90.8(2)	N(23)-Fe(3)-N(32)	90.7(3)
N(8)-Fe(1)-N(14)	92.7(2)	N(23)-Fe(3)-N(11)	90.7(2)
N(2)-Fe(1)-N(14)	91.3(2)	N(32)-Fe(3)-N(11)	88.0(3)
N(8)-Fe(1)-N(3)	93.0(2)	N(23)-Fe(3)-N(24)	80.4(2)
N(2)-Fe(1)-N(3)	80.8(2)	N(32)-Fe(3)-N(24)	92.8(2)
N(14)-Fe(1)-N(3)	170.3(2)	N(11)-Fe(3)-N(24)	171.1(2)
N(8)-Fe(1)-N(15)	171.9(2)	N(23)-Fe(3)-N(12)	92.7(2)
N(2)-Fe(1)-N(15)	93.4(2)	N(32)-Fe(3)-N(12)	168.6(2)
N(14)-Fe(1)-N(15)	80.2(2)	N(11)-Fe(3)-N(12)	81.1(2)
N(3)-Fe(1)-N(15)	94.6(2)	N(24)-Fe(3)-N(12)	98.6(2)
N(8)-Fe(1)-N(9)	81.4(2)	N(23)-Fe(3)-N(33)	171.1(2)
N(2)-Fe(1)-N(9)	171.9(2)	N(32)-Fe(3)-N(33)	80.8(3)
N(14)-Fe(1)-N(9)	91.3(2)	N(11)-Fe(3)-N(33)	91.4(2)
N(3)-Fe(1)-N(9)	97.3(2)	N(24)-Fe(3)-N(33)	97.4(2)
N(15)-Fe(1)-N(9)	94.7(2)	N(12)-Fe(3)-N(33)	96.2(2)
N(5)-Fe(2)-N(20)	91.6(2)	N(17)-Fe(4)-N(29)	88.4(2)
N(5)-Fe(2)-N(26)	91.6(2)	N(17)-Fe(4)-N(35)	88.7(3)
N(20)-Fe(2)-N(26)	90.0(2)	N(29)-Fe(4)-N(35)	89.6(2)
N(5)-Fe(2)-N(6)	81.2(2)	N(17)-Fe(4)-N(36)	169.7(3)
N(20)-Fe(2)-N(6)	172.6(2)	N(29)-Fe(4)-N(36)	94.2(2)
N(26)-Fe(2)-N(6)	91.8(2)	N(35)-Fe(4)-N(36)	81.4(3)
N(5)-Fe(2)-N(21)	93.5(3)	N(17)-Fe(4)-N(30)	93.9(3)
N(20)-Fe(2)-N(21)	81.3(2)	N(29)-Fe(4)-N(30)	80.3(2)
N(26)-Fe(2)-N(21)	170.0(2)	N(35)-Fe(4)-N(30)	169.4(3)

N(6)-Fe(2)-N(21)	97.5(2)	N(36)-Fe(4)-N(30)	96.3(3)
N(5)-Fe(2)-N(27)	172.1(3)	N(17)-Fe(4)-N(18)	80.7(3)
N(20)-Fe(2)-N(27)	90.2(2)	N(29)-Fe(4)-N(18)	168.4(3)
N(26)-Fe(2)-N(27)	80.7(3)	N(35)-Fe(4)-N(18)	94.3(2)
N(6)-Fe(2)-N(27)	97.1(2)	N(36)-Fe(4)-N(18)	97.2(3)
N(21)-Fe(2)-N(27)	94.4(3)	N(30)-Fe(4)-N(18)	96.2(3)
		cage (*S*)-3	
Fe(1)-N(8)	1.916(6)	Fe(2)-N(5)	1.952(5)
Fe(1)-N(11)#3	1.919(6)	Fe(2)-N(5)#3	1.952(5)
Fe(1)-N(2)	1.928(6)	Fe(2)-N(5)#4	1.952(5)
Fe(1)-N(12)#3	1.995(6)	Fe(2)-N(6)	1.987(5)
Fe(1)-N(3)	1.998(6)	Fe(2)-N(6)#3	1.987(5)
Fe(1)-N(9)	2.028(6)	Fe(2)-N(6)#4	1.987(5)
N(8)-Fe(1)-N(11)#3	90.4(3)	N(5)-Fe(2)-N(5)#3	90.7(2)
N(8)-Fe(1)-N(2)	91.2(2)	N(5)-Fe(2)-N(5)#4	90.7(2)
N(11)#3-Fe(1)-N(2)	90.6(2)	N(5)#3-Fe(2)-N(5)#4	90.7(2)
N(8)-Fe(1)-N(12)#3	170.4(3)	N(5)-Fe(2)-N(6)	80.6(2)
N(11)#3-Fe(1)-N(12)#3	80.9(3)	N(5)#3-Fe(2)-N(6)	92.3(2)
N(2)-Fe(1)-N(12)#3	93.1(2)	N(5)#4-Fe(2)-N(6)	170.8(2)
N(8)-Fe(1)-N(3)	92.1(2)	N(5)-Fe(2)-N(6)#3	170.8(2)
N(11)#3-Fe(1)-N(3)	172.1(3)	N(5)#3-Fe(2)-N(6)#3	80.6(2)
N(2)-Fe(1)-N(3)	81.9(2)	N(5)#4-Fe(2)-N(6)#3	92.3(2)
N(12)#3-Fe(1)-N(3)	97.0(2)	N(6)-Fe(2)-N(6)#3	96.71(19)
N(8)-Fe(1)-N(9)	80.0(3)	N(5)-Fe(2)-N(6)#4	92.3(2)
N(11)#3-Fe(1)-N(9)	91.5(2)	N(5)#3-Fe(2)-N(6)#4	170.8(2)
N(2)-Fe(1)-N(9)	170.9(3)	N(5)#4-Fe(2)-N(6)#4	80.6(2)
N(12)#3-Fe(1)-N(9)	95.9(3)	N(6)-Fe(2)-N(6)#4	96.71(19)
N(3)-Fe(1)-N(9)	96.2(2)	N(6)#3-Fe(2)-N(6)#4	96.71(19)

For **(*R*)-1**: #1 -x+y,-x,z #2 -y,x-y,z #3 -x+y-1,-x+1,z #4 -y+1,x-y+2,z #5 -x+y+2,-x+1,z #6 -y+1,x-y-1,z

For **(*S*)-1**: #1 -x+y+1,-x+1,z #2 -y+1,x-y,z #3 -y,x-y,z #4 -x+y,-x,z

For **(*S*)-3**: #1 -y+1,x-y-1,z #2 -x+y+2,-x+1,z #3 -x+y,-x,z #4 -y,x-y,z #5 -x+y+1,-x+2,z #6 -y+2,x-y+1,z

11. References

1 *SAINT-Plus*, version 6.02; Bruker Analytical X-ray System: Madison, WI, 1999.

2 G. M. Sheldrick, *SADABS An empirical absorption correction program*; Bruker Analytical X-ray Systems: Madison, WI, 1996.

3 G. M. Sheldrick, *SHELXTL-97*; Universität of Göttingen: Göttingen, Germany, 1997.